

# Effect of size on the shear strength between old to new concrete interface

S. Cattaneo & M. Scamardo

*Department of Architecture, Built Environment and Construction Engineering, Politecnico di Milano, Milan, Italy*

**ABSTRACT:** The retrofitting of the existing RC structures with added concrete layer crossed by post installed rebars is strongly related to the behavior of the interface between the new and the old concretes. The overall strength of the connection depends on several mechanisms such as friction and dowel action between the two concrete layers as well as the type of loading. In the past, attention was given to understand these mechanisms considering several types of specimens, usually characterized by small dimensions. Nevertheless, it is well known that size effect is often crucial in concrete elements. In this paper, with reference to a specimen geometry already employed for assessing the shear strength between old to new concrete interface, the influence of the size effect on the overall response is analyzed. Based on the results of an experimental campaign, a numerical model is adopted and validated. Therefore, specimens with three different dimensions were numerically analyzed to define the suitable specimen size.

## 1 INTRODUCTION

Connections between concrete layers with different ages are very common in both existing buildings (i.e. repairing or strengthening) and in new buildings (e.g. connecting pre-cast elements) (Júlio et al. 2005). To ensure a reliable functioning of these connections, a quantifiable amount of shear strength at the interface must be mobilized.

The shear transfer mechanism between two concrete layers is a very complex phenomenon influenced by several interacting parameters (Mattock et al. 1975, Bass et al. 1989, Júlio et al. 2005, 2010, Santos & Júlio 2012, Cattaneo et al. 2021, Palieraki et al. 2021): (1) the quality, the strengths and also the thickness of the two layers (new and old); (2) the surface of the old concrete that could be smooth or artificially roughened; (3) the diameter of the reinforcement crossing the interface; (4) the reinforcement ratio crossing the interface; (5) the embedment length into old/new concrete; (6) external actions on the structure; (7) type of actions (monotonic/cyclic and the amplitude of the displacement); (8) the size of the shear interface. For these reasons, several research campaigns have been carried out in the past (Mattock et al. 1975, Bass et al. 1989, Júlio et al. 2005, 2010, Santos & Júlio 2012, Cattaneo et al. 2021, Palieraki et al. 2021) to evaluate the effect of each parameter and their interactions. Most of the studies were based on monotonic loading experimental tests, while in actual cases (i.e. bridge decks, jacketed columns) structures undergo reversal cyclic loading, e.g., due to fatigue or seismic actions.

For this reason, recently the European Organization for Technical Assessment (EOTA) introduced a new European Assessment Document (EAD) (EOTA 2021) that allows to evaluate the shear strength both under monotonic and cyclic actions. The EAD defines an experimental set-up to assess the shear strength (considering also reversal cyclic loads) that was designed to reduce the perturbative effects of the boundary conditions and of parasitic bending moments. Although the proposed set-up seems to be the most reliable (Cattaneo et al. 2021), the parasitic effects are not eliminated, and the specimen dimensions are relatively of large size with respect to the most common dimensions which usually range between 50 and 100 cm (with length from 30 cm) (Wieneke 2019), and require a significant experimental

effort. Nevertheless, it is well known that concrete is a quasi-brittle material, because the size effect could play a crucial effect in assessing the real shear strength (Biolzi et al. 2000).

The aim of this paper is to investigate the influence of the specimen size on the overall behavior. A numerical model of the specimen defined in the EAD (EOTA 2021) was developed and validated on the basis of experimental result. Two additional models were made considering reduced length of the specimen with respect to the length of the reference specimen (ratio between interface area/reference area 1:0.5:0.25).

## 2 EXPERIMENTAL RESEARCH

### 2.1 Test specimen and test set-up

An experimental campaign aimed at assessing the shear strength according to EAD (EOTA 2021) was carried out (Cattaneo et al. 2021), considering the geometry shown in Figure 1. The specimens were realized in two phases: the green block, casted first, simulates the existing concrete, while the grey block, casted at a second stage, represents the added concrete. The concrete strengths were evaluated at the time of testing on cubes (side 150 mm). The average compressive strength of the old concrete was about 28.4 MPa and of the new concrete was 32.1 MPa. The interface (area 200 mm x 500 mm) was crossed by three concrete screws (diameter 14 mm, length 150 mm,  $f_{yk} = 690$  MPa). After three months from the first casting, the interface surface (500 x 200 mm) was artificially roughened with the use of an electric chisel by employing different bits. The average roughness of the interface was 2.98 mm, measured with the sand-patch method according to (EN 13036-1:2010 2010). In the roughened area three concrete screws (Figure 1, in red) were installed with a spacing of 170 mm, and with an embedment depth in the old concrete of 85 mm (65 mm in the new concrete). Overall, 4 specimens were tested.

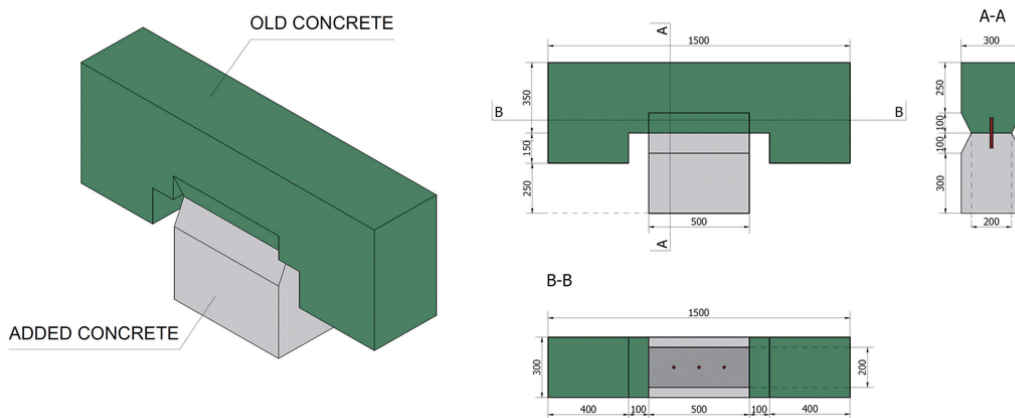


Figure 1. Specimen geometry.

Figure 2 shows the test set-ups. The specimen was set on the strong floor and restrained on both sides (front and back) with two stiff supports connected to the strong floor. The load was applied at the interface level with two plates and four rods that connected the specimen to the hydraulic jack (with capability of 500 kN equipped with a load cell of 500 kN).

Two additional orthogonal restraints were added to allow the sliding of the “old concrete block”, preventing rotations. Four steel cylinders (two on both side of the specimen) were added at the bottom to support the specimen. Similarly, on the top of the specimen, four steel cylinders support two steel plates that were connected to the strong floor to prevent the rotation of the specimen. A Teflon sheet was placed between steel cylinders and concrete surface to reduce friction. The slip between the old and the new concrete block was measured with four LVDTs (gage length 10 mm) placed close to the interface. All measurements were acquired with the MOOG system. The tests were displacement controlled with monotonic loading.



Figure 2. Experimental test set-up.

## 2.2 Test results

The average shear strength was 3.7 MPa with a coefficient of variation of about 9.5%. A typical load-displacement curve is shown in Figure 3, in which distinct phases are clearly identifiable: the elastic branch (up to point A), the cracking of the interface between the two concrete castings (between points A and B), the friction and dowel action effect (associated to the plateau starting from point B). This curve was used to calibrate the parameters of the numerical model.

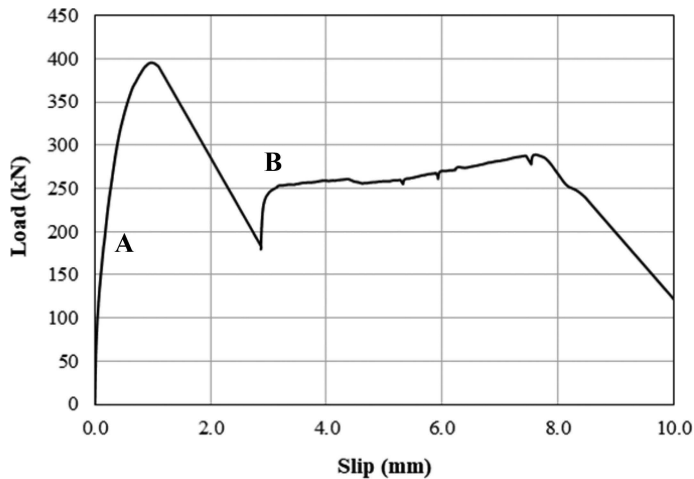


Figure 3. Load-displacement curve.

## 3 NUMERICAL ANALYSES

Three different specimens were modeled with the software ABAQUS (Dassault Systèmes 2017) to assess the influence of the size effect on the overall mechanical response. The reference specimen size was assumed according to EAD (EOTA 2021) as in Figure 1, with a shear interface area of 500 mm x 200. The scaled specimens (Figure 4) had the same thickness and reduced length and height (1:0.5:0.25), resulting in shear interface areas of 250 mm x 200 mm and 125 mm x 200 mm. A higher reinforcement percentage has been adopted in the scaled specimens with respect to the reference one (0.61% vs. 0.46%) in order to have an integer number of connectors.

The mesh was created using an automatic tool with some manual refinement (Figure 5, left). The interface between the concrete parts was modelled as a concrete layer with a thickness of 10 mm (Cattaneo et al. 2021). The top and bottom concrete blocks, the interface layer and the anchors were modeled with linear hexahedral elements (type C3D8). The element size ranges from approximately 1.5 mm in regions that require more refinement, such as near the anchors, to around 20 mm in regions that allow a rougher mesh (far from stress concentration). The reinforcement used for the cage of the specimen according to (EOTA 2022) (diameters 8 mm

and 12 mm) was modeled as 1D elements (linear line elements of type B31). As these elements do not require much refinement, their meshes reach element sizes up to 50 mm.

The boundary conditions were defined with the aim to reproduce the experimental settings (Figure 5, right). The new concrete block was fixed on the lateral surfaces of the specimen. Orthogonal constraints were considered at the top of the old concrete, to prevent the rotations and to allow the sliding of the old/new concrete blocks. The top and bottom surfaces of the interface layer were tied to the old and new concrete, respectively (no relative motion allowed). A perfect bond was considered between the anchors and the surrounding concrete, defined as surface-to-surface contact with tangential behavior (friction coefficient  $\mu=0.8$ ) and normal behavior (hard contact). The horizontal displacement was applied on the side of the old concrete block.

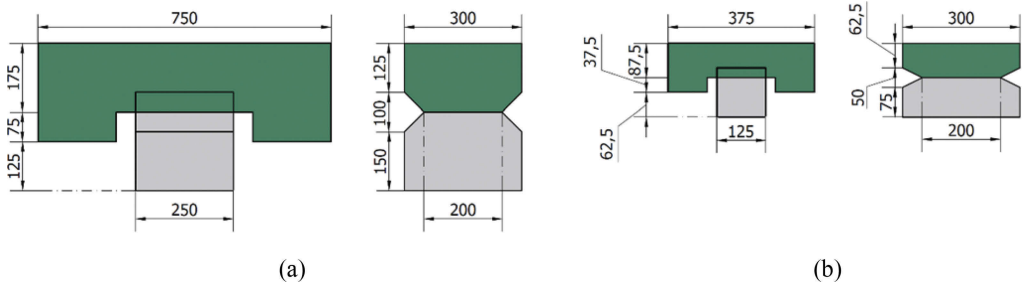


Figure 4. Scaled specimens geometry: (a) size II and (b) size III.

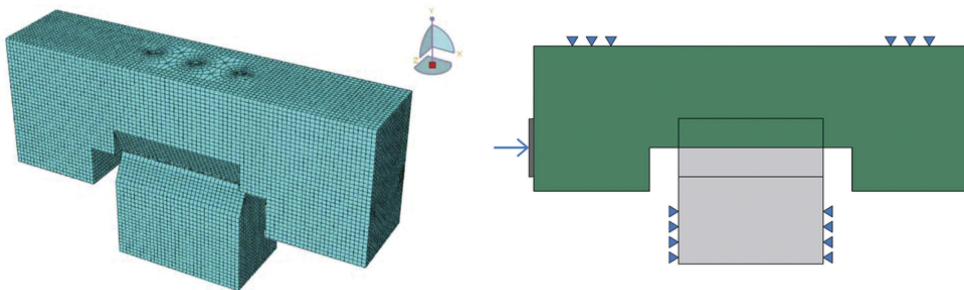


Figure 5. FEM mesh (left) and boundary conditions (right).

### 3.1 Model validation

The validation of the numerical model was performed by comparing the numerical results of the reference specimen with the experimental results (Cattaneo et al. 2021). The nonlinear behavior of the concrete was taken into account by assuming the Concrete Damaged Plasticity (CDP) model (Lubliner et al. 1989, Dassault Systèmes 2017) as constitutive law. The elastic modulus  $E_c$  was assumed equal to 31 GPa (C20/25) and 32 GPa (C28/35) for the old and the new concrete, respectively. The adopted Poisson's ratio had a value of 0.18 for both materials. A lower value of elastic modulus was chosen for the interface ( $E_c = 1$  GPa), as proposed in other researches (Cattaneo et al. 2021).

The parameters adopted for the CDP are summarized in Table 1 where  $\Psi$  is the dilation angle,  $e$  is the eccentricity,  $f_{b0}/f_{c0}$  represents the ratio between strengths in biaxial compression and in uniaxial compression,  $K$  represents the ratio between deviatoric stresses in uniaxial tension and compression (in absolute values) and  $\mu$  represents the viscosity. The values were calibrated on the experimental results and according to typical values proposed in the scientific literature (Lubliner et al. 1989). Figure 6 shows the good agreement between the experimental and the numerical load-displacement curves comparison.

Table 1. CDP Parameters.

| $\Psi(^{\circ})$ | e   | $f_{b0}/f_{c0}$ | K     | $\mu$  |         |
|------------------|-----|-----------------|-------|--------|---------|
|                  |     |                 |       | C25/30 | C28/35  |
| 15               | 0.1 | 1.16            | 0.667 | 0.006  | 0.00205 |

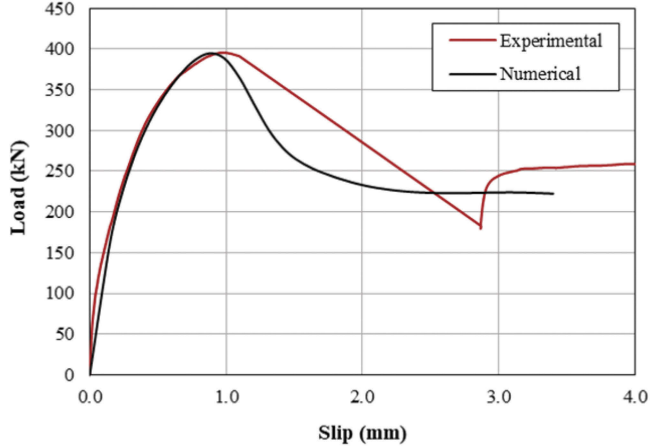


Figure 6. Numerical and experimental load-displacement curves.

### 3.2 Numerical results

The load-displacement curves for the three considered sizes are shown in Figure 7a together with the experimental outcome. Figure 7b shows the variation of the average shear strength for the different contact area of the three specimens.

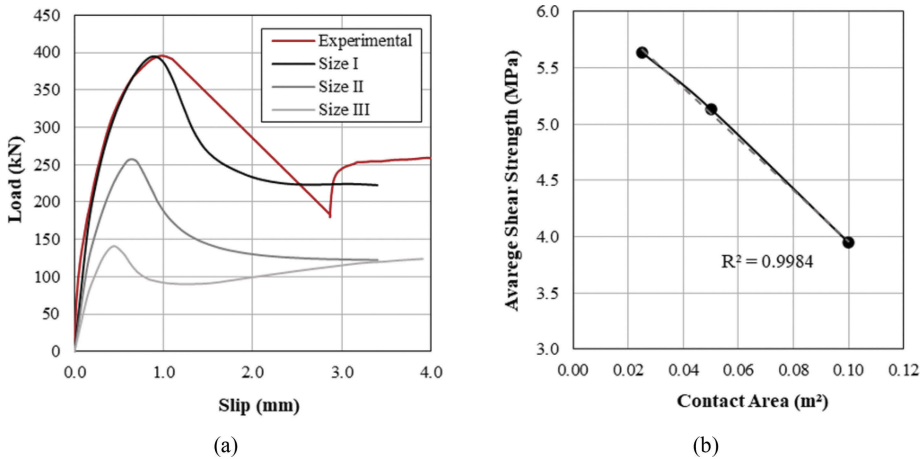


Figure 7. (a) Load-slip curves of different sizes and (b) variation of the average shear strength.

Table 2 summarizes the peak load and the associated displacement, together with the shear strength evaluated assuming a uniform stress distribution over the interface surface. As expected, the nominal shear strength decreases with increasing size, and a softer post-peak branch is observed in small specimen. These two observations confirm that this type of test is strongly size dependent (Biolzi et al. 2000).

Table 2. Size effect: main results.

|          | Contact Area<br>[mm x mm] | Peak Load [kN] | Displacement associated<br>to Peak Load [mm] | Average Shear<br>Strength [MPa] |
|----------|---------------------------|----------------|--|---------------------------------|
| Size I   | 500 x 200                 | 394.81         | 0.878  | 3.95                            |
| Size II  | 250 x 200                 | 256.77         | 0.617  | 5.14                            |
| Size III | 125 x 200                 | 140.96         | 0.438  | 5.64                            |

It should be observed that to consider feasible specimens, 3 2 and 1 anchor were used respectively for the different sizes. This implies that the larger specimen has a lower geometric reinforcement ratio than the other two specimens in which the ratio is constant. Nevertheless, the higher reinforcement ratio affects mainly the dowel action (i.e. post peak behavior). Indeed, the size effect is noted also for the two specimens (II and III) with the same reinforcement ratio (Figure 7b).

#### 4 DISCUSSION

The numerical results make possible to add further considerations to the experimental issues. By considering the distribution of the tensile damage at the peak load in a section at a quarter of the width (Figure 8), it is possible to observe that the reference specimen (a) and the medium specimen (b) show non-uniform damage distribution, while the smaller specimen (c) shows a more uniform damage distribution. This is probably due to the fact that, in the bigger specimens, the eccentricity between the applied load (that acts at the interface level) and the respective horizontal reaction force (that is located on the new concrete part at a distance of about 25 cm) is higher than in the smaller specimen. Indeed, on the side of the reaction (Figure 8a) a certain damage appears close to the support reaction.

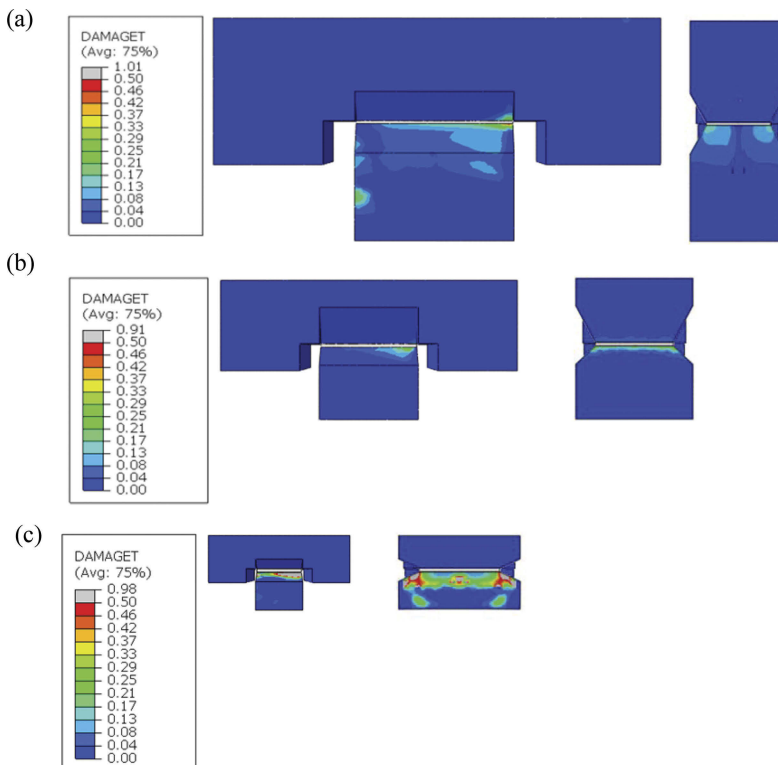


Figure 8. Distribution of tensile damage for (a) size I, (b) size II and (c) size III models.

Looking at the shear stress distribution (Figure 9), it is interesting to observe that all sizes exhibit similar distribution with a concentration of stresses close to the loaded edge, high stresses close to the anchor position which drop in the anchor section. Although the trend is similar, in the reference specimen there is a high stress concentration close to the edge of the specimen and then, in the intermediate section, there is a nearly uniform stress distribution. The smaller specimen shows the higher stress close to the edge, while the intermediate size has the lower stress close to edge. Overall, the stress distribution of the intermediate specimen does not show steep changes, although there is not an area with constant stress (as shown in the central portion of the reference specimen).

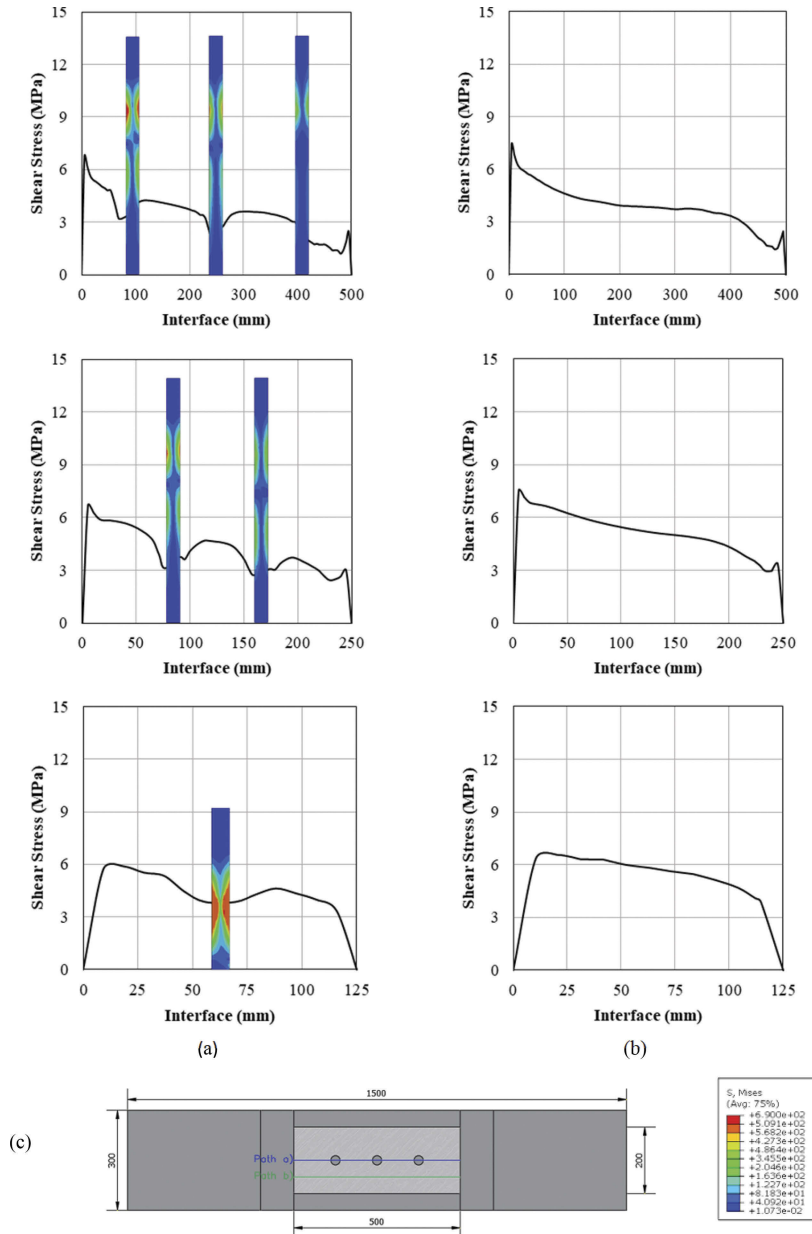


Figure 9. Shear stress distribution in path a (a) and in path b (b) for the three different sizes, with Von Mises Stresses in the anchor. In (c) section scheme with anchor stresses legend.

Based on the obtained results, it is evident how stress and damage distributions are strongly influenced by the size of the specimen and higher stress gradients are found when the size effect is more pronounced. In any case, at the interface, a non-uniform stress distribution is manifest with a mixed-mode stress field which affects the damage evolution and the experimental results (Biolzi 1990). Although the smaller specimen leads to the highest strength and thus it is not on the safe side, it shows a more uniform stress distribution. The intermediate specimen leads to higher strength with respect to the reference specimen, and, although the stress distribution is not uniform, it does not present steep changes. The reference specimen allows to evaluate the shear strength on the safe side.

## 5 CONCLUSIONS

The numerical analyses conducted highlight that the assessment of the shear strength is strongly affected by the size effect both in terms of shear stress distribution, strength and ductility.

The reference specimen seems a suitable specimen size for a safer evaluation of the shear strength. The intermediate specimen could be considered to assess the shear strength, since the stress distribution along the interface does not show steep changes. In this case, a suitable reduction coefficient should be applied to account for the size effect and a proper experimental validation is needed. The smaller specimen does not seem suitable to assess the shear strength, since it is strongly affected by the size effect. Moreover, the fact that the new cast part resulted strongly damaged suggests that secondary effects could be involved in the strength evaluation.

## REFERENCES

- Bass, R.A., Carrasquillo, R.L., & Jirsa, J.O., 1989. Shear transfer across new and existing concrete interfaces. *ACI Structural Journal*, 86 (4).
- Biolzi, L., 1990. Mixed mode fracture in concrete beams. *Engineering Fracture Mechanics*, 35 (1–3).
- Biolzi, L., Cattaneo, S., & Guerrini, G.L., 2000. Fracture of Plain and Fiber-Reinforced High Strength Mortar Slabs with EA and ESPI Monitoring. *Applied Composite Materials*, (7), 1–12.
- Cattaneo, S., Zorzato, G., & Bonati, A., 2021. Assessing method of shear strength between old to new concrete interface under cycling loading. *Construction and Building Materials*, 309.
- Dassault Systèmes, 2017. ABAQUS/CAE Documentation.
- EN 13036-1:2010, 2010. *Road and airfield surface characteristics - Test methods - Part 1: Measurement of pavement surface macrotexture depth using a volumetric patch technique*.
- EOTA, 2021. *EAD 332347-00-0601-v01: Connector for strengthening of existing concrete structures by concrete overlay: behavior under seismic action*.
- EOTA, 2022. *EAD 330076-01-0604-v01: Metal injection anchors for use in masonry under seismic actions*. Brussels, Belgium.
- Júlio, E., Branco, F., & Silva, V., 2005. Reinforced concrete jacketing - Interface influence on monotonic loading response. *ACI Structural Journal*, 102 (2).
- Júlio, E., Dias-da-Costa, D., Branco, F., & Alfaiate, J., 2010. Accuracy of design code expressions for estimating longitudinal shear strength of strengthening concrete overlays. *Engineering Structures*, 32 (8).
- Lubliner, J., Oliver, J., Oller, S., & Oñate, E., 1989. A plastic-damage model for concrete. *International Journal of Solids and Structures*.
- Mattock, A.H., Johal, L., & Chow, H.C., 1975. Shear transfer in reinforced concrete with moment or tension acting across the shear plane. *J Prestressed Concr Inst*, 20 (4).
- Palieraki, V., Vintzileou, E., & Silva, J.F., 2021. Behavior of RC interfaces subjected to shear: State-of-the art review. *Construction and Building Materials*.
- Santos, P.M.D. & Júlio, E.N.B.S., 2012. A state-of-the-art review on shear-friction. *Engineering Structures*.
- Wieneke, K.M., 2019. Horizontal Shear Design of Concrete Interfaces in Beam and Slab Structures. *PhD Thesis*.